Automated Detection of Chondrocytes in Growth Plate Images

Emily Beylerian, Brian de Silva, Ben Gross, Hannah Kastein
Mentors: Dr. Maria-Grazia Ascenzi and Hayden Schaeffer

UCLA Applied Mathematics REU 2012

Growth Plates

Bones

- Longitudinal bone growth via growth plates
- Chondrocytes arranged in vertical columns
- Cell division causes growth

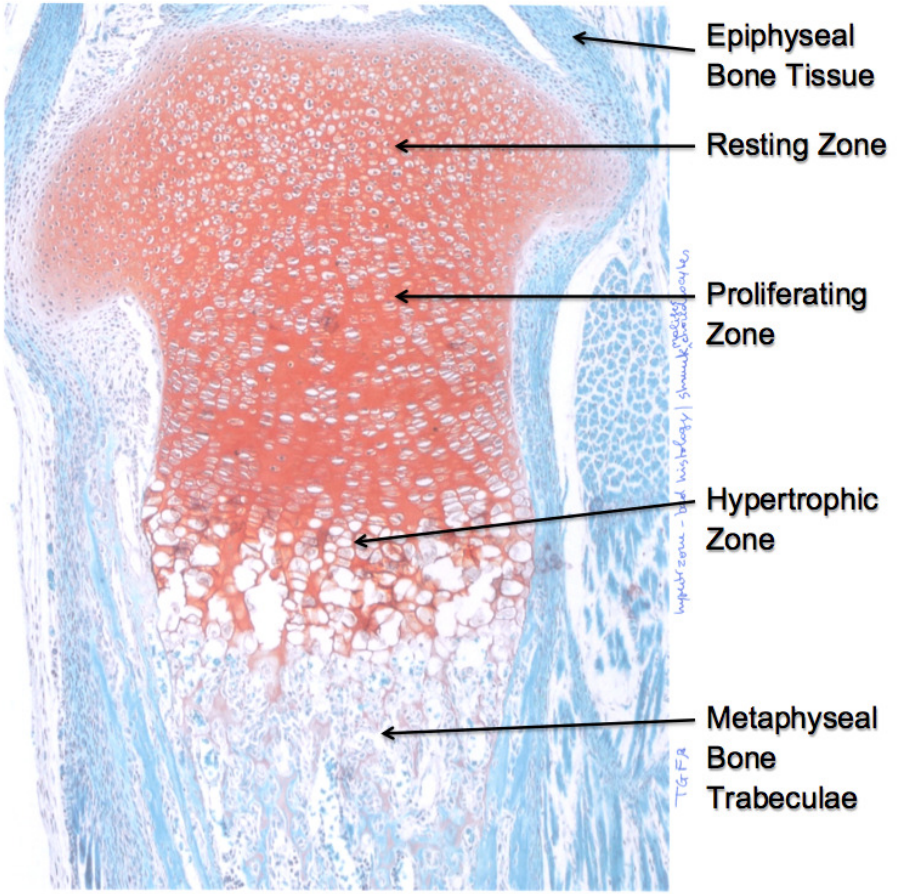

Our Project

Disorders in the Growth Plate

- Misaligned chondrocytes stunt growth
- Alignment depends on genetic factors

Our Goals

- Develop automated image processing software
- Compare normal and abnormal growth plates

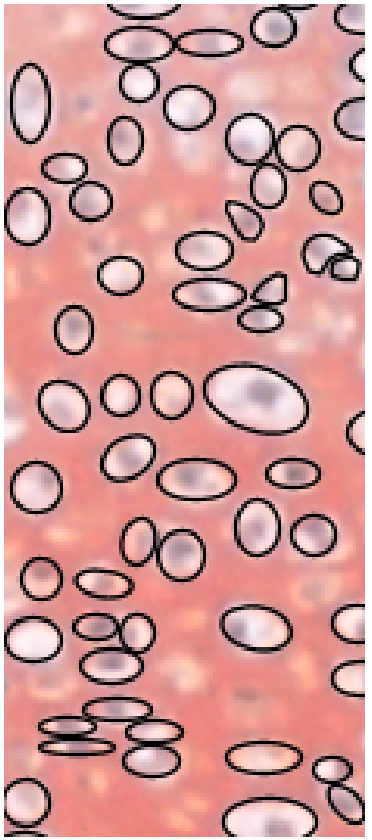

Image Processing

- Want to extract cell locations from matrices of intensity values

Challenges

- Cells beneath plane of focus
- Inconsistencies across image
  - Cell size/shape
  - Appearance of nuclei
  - Stain penetration in background

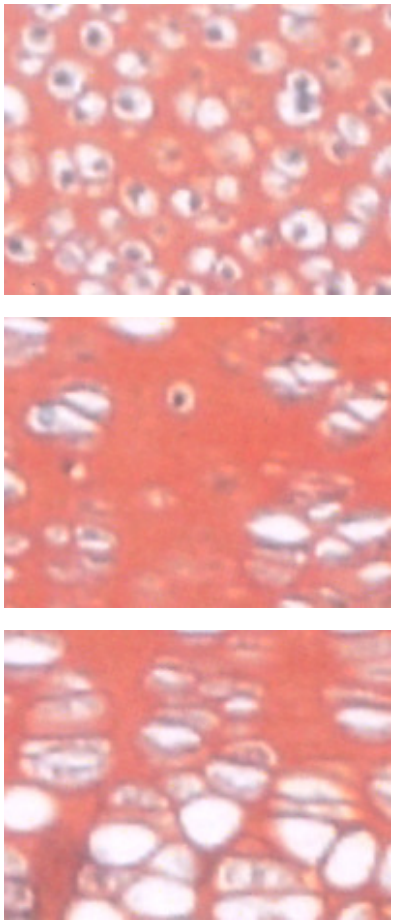

Pre-Existing Methods

Software

- ImageJ
- CellProfiler
- High-throughput and high-content screening (HT-HCS)

Methods

- Segmentation
- Cartoon-Texture Decomposition
- K-Means Clustering
- Spectral Clustering

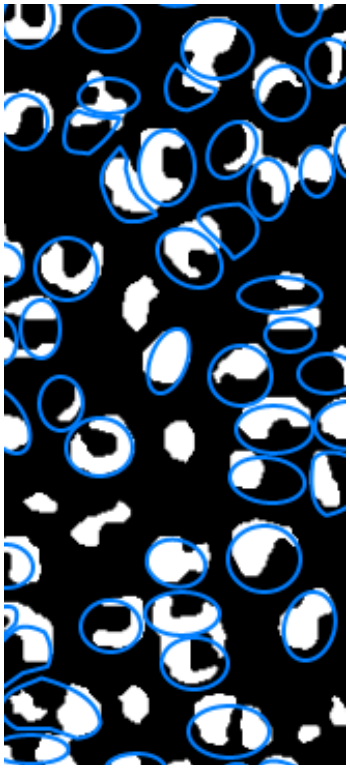

Manual detections (blue) overlaid on texture decomposition

Algorithm

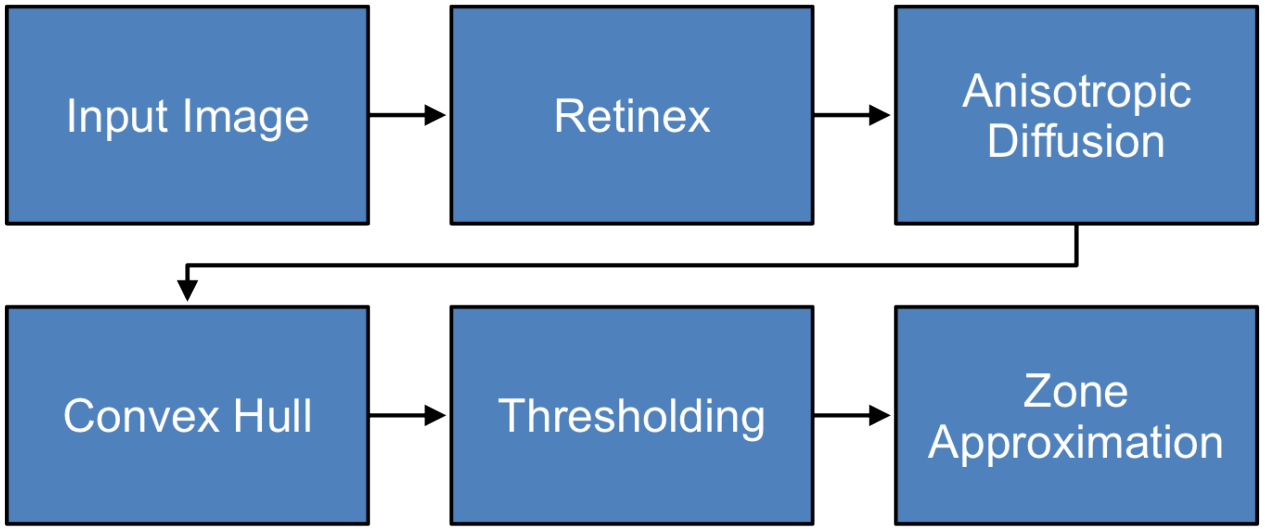
Input Image
Retinex
Anisotropic Diffusion
Convex Hull
Thresholding
Zone Approximation

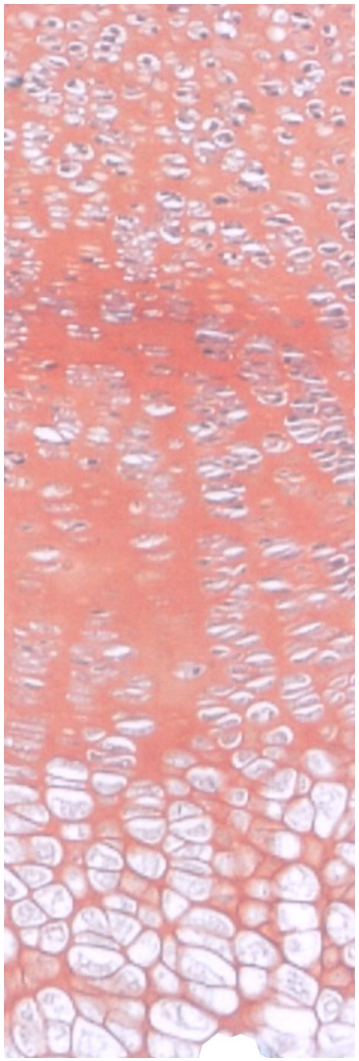

Retinex: A Color Contrast Algorithm

- Attempt to imitate and describe human color perception
- Smooths together subtle variations in shading
- Remove cells outside plane of focus

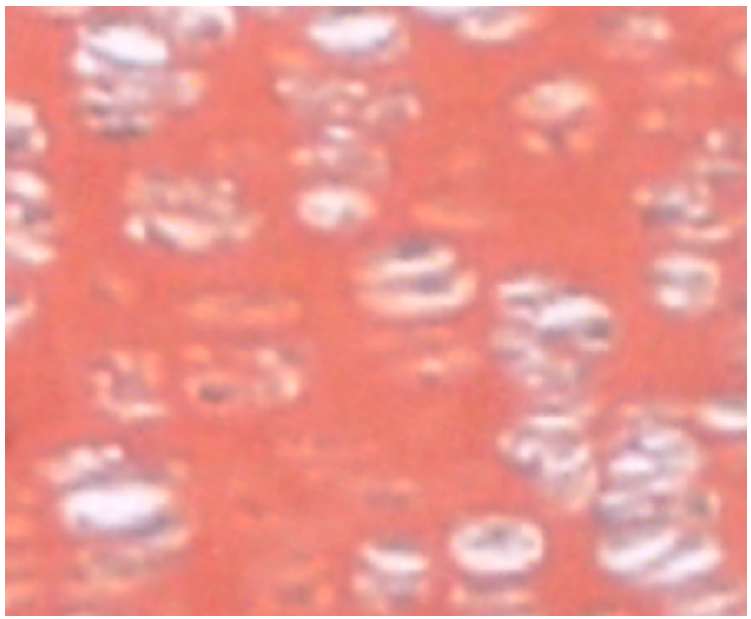

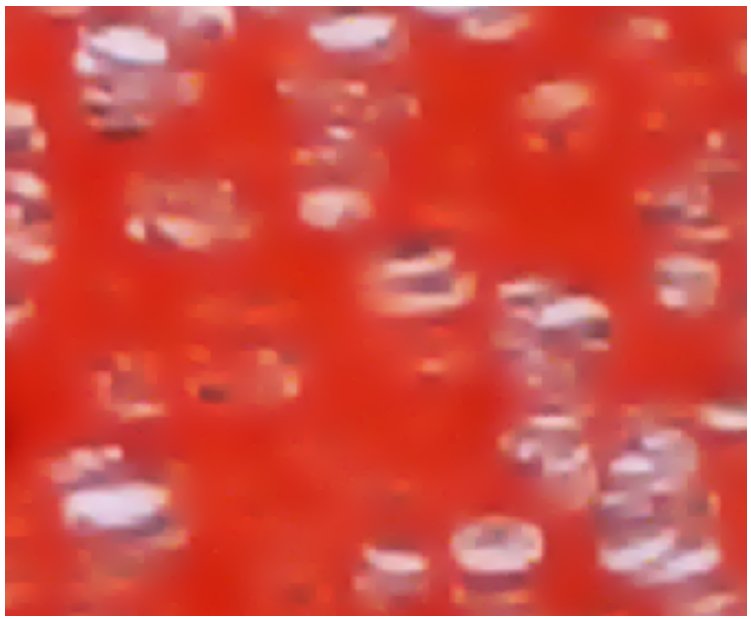

Retinex cont.

Given an initial image, f, finds a reconstructed image, u, such that

$$-\Delta u_{i,j} = F_{i,j}$$

Where

$$\Delta u_{i,j} = u_{i+1,j} + u_{i-1,j} + u_{i,j+1} + u_{i,j-1} - 4u_{i,j}$$

is the discrete Laplacian at mesh point (i,j),

$$F_{i,j} = T(f_{i,j} - f_{i+1,j}) + T(f_{i,j} - f_{i-1,j}) + T(f_{i,j} - f_{i,j+1}) + T(f_{i,j} - f_{i,j-1})$$

and T is a thresholding function such that

$$T(x) = \begin{cases} 0 & \text{if} \quad |x| \leq \tau \\ x & \text{if} \quad |x| > \tau \end{cases}$$

Anisotropic Diffusion

Cartoon

Gradient

$$\min_u \int \Psi\left(\nabla u, \nabla u^T\right) dx$$

$$g\left(|\nabla u|\right) = \frac{1}{|\nabla u|^p}$$

- Related to Perona-Malik Diffusion
- Both nonlocal and nonlinear
- Emphasis on preserving edges

Morphological Functions

Convex Hull

- Fits polygon to cell outline
- Connects discontinuities linearly
- Need separation between cells

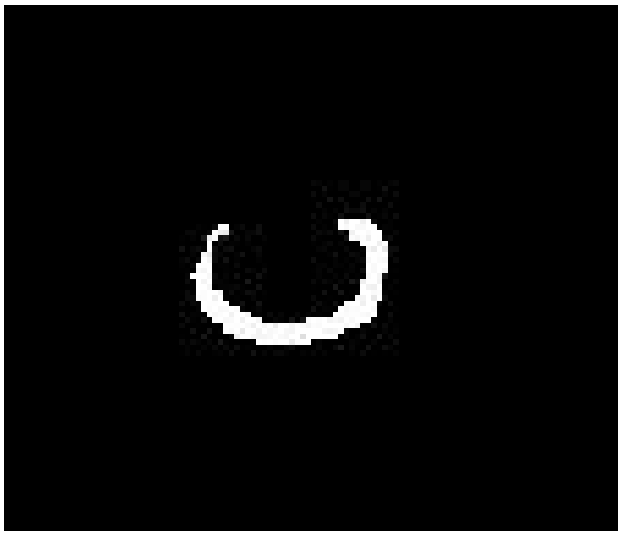

Morphological Functions

Size Thresholding

Shape Thresholding

- Isoperimetric Inequality

$$\frac{4\pi A}{L^2}$$

- Relationship between shape area and circumference
- Ratio equals one for circle

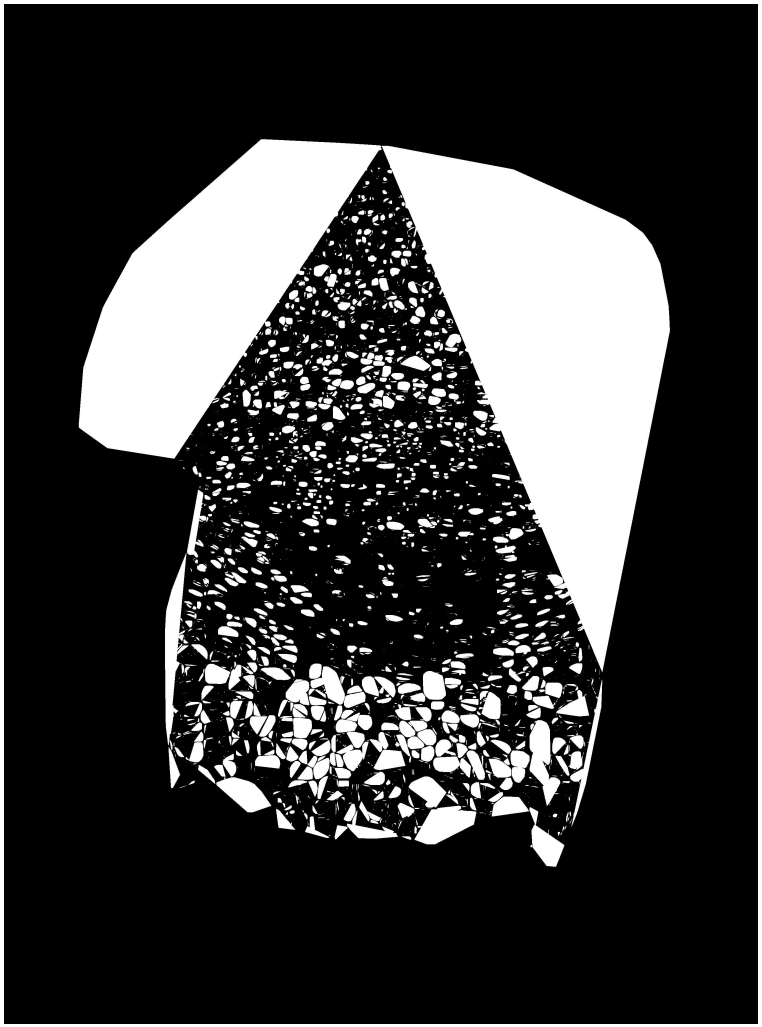

Automated Growth Plate Zone Detection

- Classify each object by its Isoperimetric Ratio ($\frac{4\pi A}{L^2}$)
- Plot object location vs. Ratio and approximate graph with a fourth degree polynomial
- Inflection points at zone boundaries

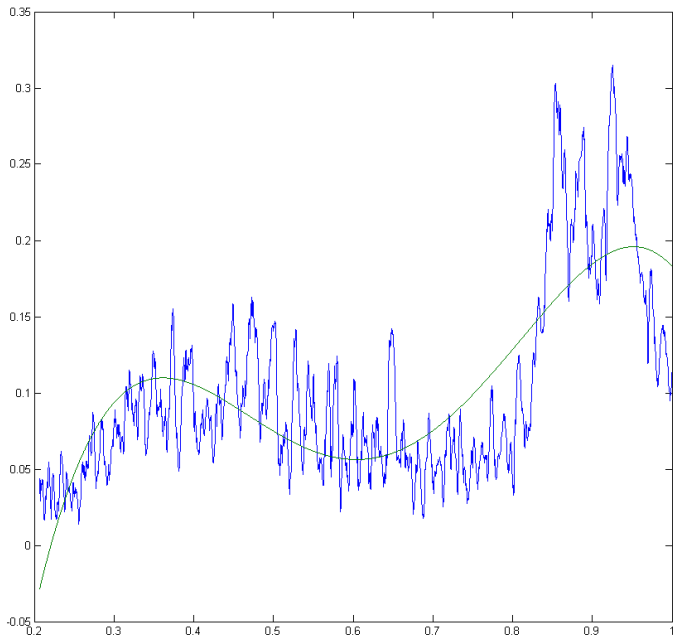

Results

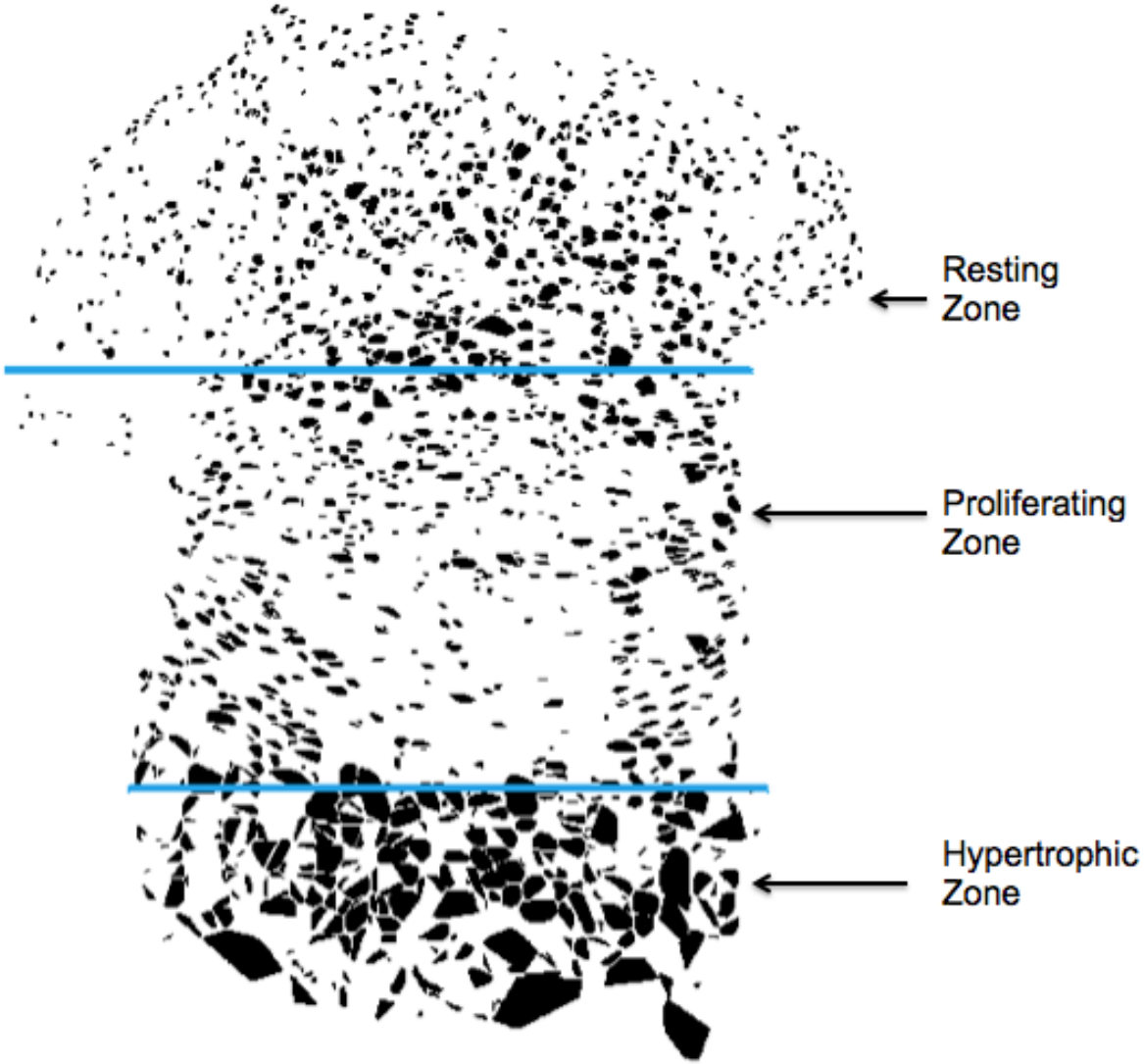

Results

Algorithm Detections

Manual Detections

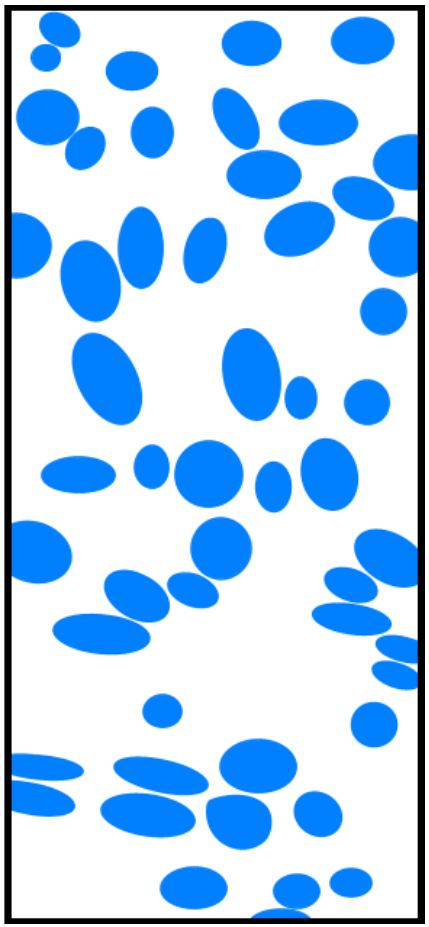

Results

Original Growth Plate

Overlay of Final Output

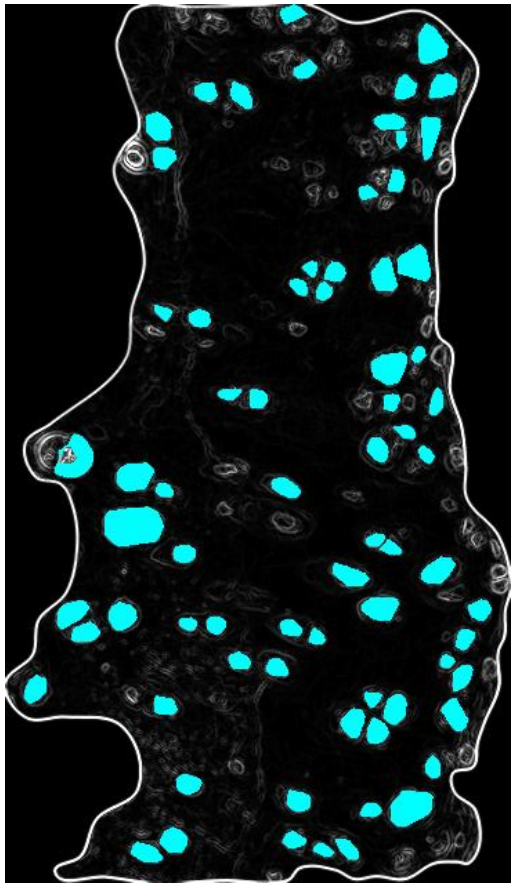

Clustering Error Statistics

Error Analysis

- How well does our algorithm segment the cells in our images?
- Many metrics/statistics for clustering analysis

Metric Requirements

- Can compare an unequal number of clusters
- Can handle large variations in cluster sizes
- Must not be computationally complex

Error Statistics

- Classes $\{L_j\}$ in our 'ground truth' image S=$\{I_1, \ldots, I_N\}$
- Clusters $\{C_i\}$ in our segmented image $S' = \left\{I'_1, \ldots, I'_N\right\}$

Clustering Purity

- Purity=$\sum_i \frac{|C_i|}{N} max_j \frac{|C_i \cap L_j|}{|L_j|}$
- Not robust to clusters which subdivide classes, trivial clusters, or clusters that span multiple classes
- Up to 88%

Rand Indicies

- Classes $\{L_j\}$ in our 'ground truth' image S=$\{I_1, \ldots, I_N\}$
- Clusters $\{C_i\}$ in our segmented image $S' = \left\{I'_1, \ldots, I'_N\right\}$

Rand Index

- $R(S, S') = \frac{1}{\binom{N}{2}} (|A| + |B|)$
  where $A = \left\{(i,j) | i \neq j, I_i = I_j, I'_i = I'_j\right\}$ and
  $B = \left\{(i,j) | i \neq j, I_i \neq I_j, I'_i \neq I'_j\right\}$
- Compare clustering of *pairs* of pixels
- Penalizes false positives and true negatives *equally*
- Up to 74%

Conclusion

In summary, we developed a successful algorithm for:

- extraction of chondrocyte location
- zone approximations

Questions?

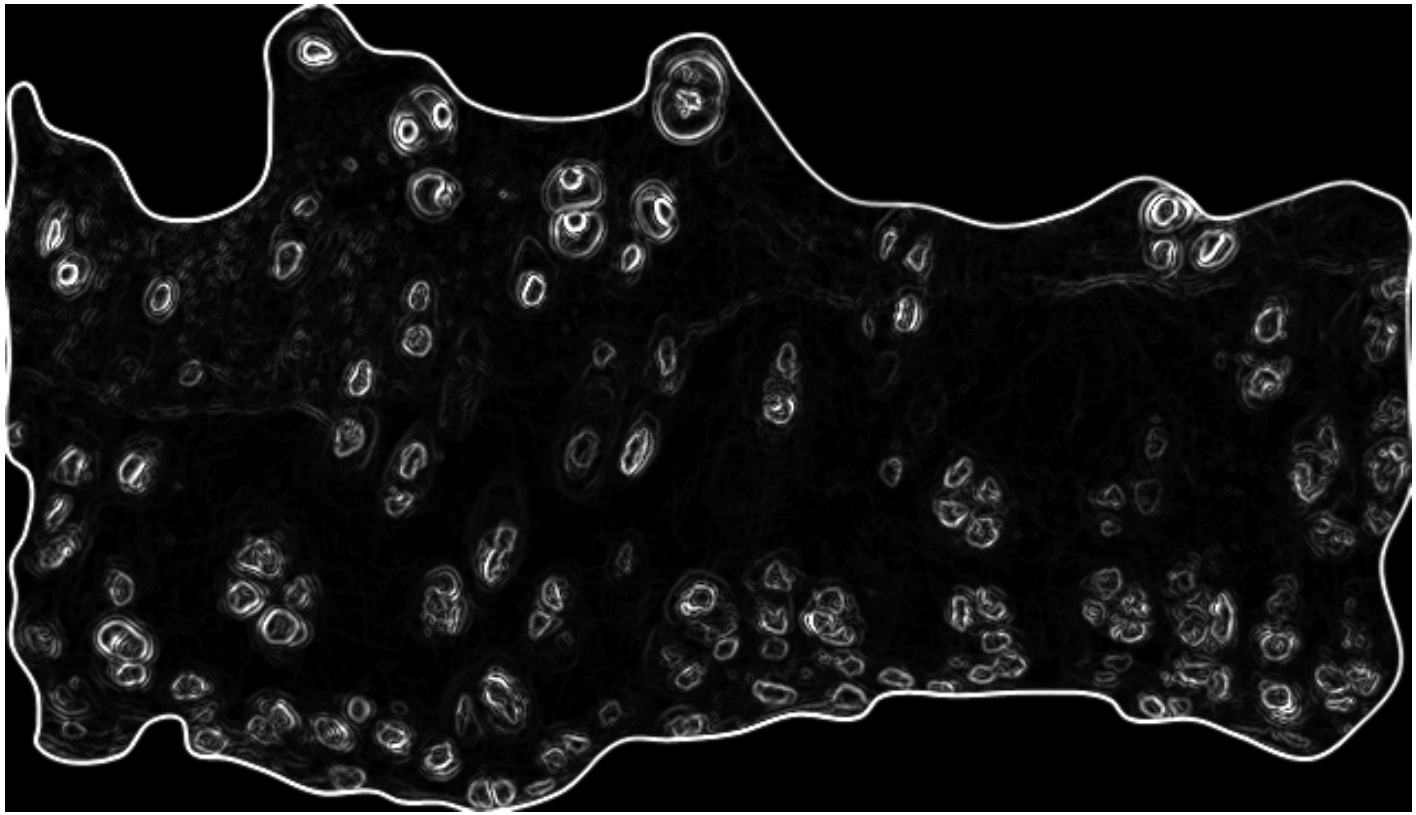

References

M-G Ascenzi, C. Blanco, I. Drayer, H. Kim, R. Wilson, K.N. Retting, K.M. Lyons, and G. Mohler. 'Effect of Localization, Length, and Orientation of Chondrocytic Primary Cilium on Murine Growth Plate Organization,' *Journal of Theoretical Biology*, 285(1):147-155, September 2011.

M-G Ascenzi, M. Lenox, and C. Farnum. 'Analysis of the Orientation of Primary Cilia in Growth Plate Cartilage: a Mathematical Model Based on Multiphoton Microscopical Images,' *Journal of Structural Biology*, 158(3):293-306, June 2007.

T. Brox, J. Weickert, B. Burgeth, and P. Mrázek. 'Nonlinear Structure Tensors,' *Universität des Saarlandes, Fachrichtung 6.1 - Mathematik*, 113, 2004.

J-M Morel, A.B. Petro, and C. Sbert. 'A PDE Formalization of the Retinex Theory,' *IEEE Transactions on Image Processing*, 2010.

J. Weickert. 'Anisotropic Diffusion in Image Processing,' *ECMI*, 1998.